J. Astrophys. Astr. (1986) 7, 83–98

Classical Cepheids and the Local Chemical Inhomogeneities in the Galactic Disc

Sunetra Giridhar *Indian Institute of Astrophysics, Bangalore 560034*

Received 1985 March 14; revised 1985 December 20; accepted 1986 January 15

Abstract. Places of formation have been derived for a sample of 23 Cepheids with well-determined atmospheric abundances in an attempt to study the chemical inhomogeneities in the local interstellar medium. The abundance data available for the sample Cepheids is compiled and critically reviewed to adopt the most reliable esimates. We find that the most conspicuous irregularity in the metallicity is exhibited by stars that are born in the local arm or in the interarm region. We propose a scenario to explain these local variations in terms of supernova-induced star formation in interstellar gas enriched by massive stars formed in the density wave.

Key words: classical Cepheids, abundances—Galaxy, chemical inhomogeneities—density-wave theory—self-propagating star formation

1. Introduction

Places of formation have been derived in the past for samples of classical Cepheids (Wielen 1973; Joshi 1982; Grivnev 1983), early-type stars (Strömgren 1967; Grosbøl 1977), and young galactic clusters (Palous *et al.* 1977) with a view to comparing the predictions of the density-wave theory with the observed spiral structure and for estimating the pattern velocity (ω_p) of the density wave. In the present investigation, however, we have used birthsites of the classical Cepheids to study the local variation of metallicity in the galactic disc.

The presence of a largescale radial abundance gradient in the disc of our Galaxy is fairly well established from the observations of H II regions, planetary nebulae and stellar atmospheres. In addition to this global variation, abundance variations across individual spiral features are also observed. Talent & Dufour (1979) have claimed steeper variations of O/H and N/H across Sagittarius, local and Perseus features compared to the global radial abundance gradient.

Giridhar (1983), while studying the radial abundance gradient in the disc of our Galaxy (using classical Cepheids as probes), found smallscale chemical inhomogeneities superposed on the largescale abundance gradient. In the present investigation, the sample is enlarged by compiling good abundance estimates, and birthsites are derived for the Cepheids of the sample to eliminate the effect of the migration of stars. The chemical inhomogeneities prevalent in various locations of the galactic disc are estimated.

The observed chemical inhomogeneities could be caused by a higher rate of star formation in certain locations of the disc. Massive stars formed there would evolve at very short timescales and enrich the interstellar medium (ISM) by the processed material very close to their birth sites. Thus, the degree of chemical enrichment of ISM depends upon the star-formation rate and on the efficiency per star-forming event to produce massive stars. We will discuss later the implications of the observed chemical inhomogeneities on various models of star formation.

In the present investigation, we have derived the places of formation for a sample of 23 Cepheids for which accurate iron abundances are known. The choice of classical Cepheids was based on their high intrinsic luminosity, young age, and the existence of good period–age and period–luminosity–colour relationships which enable one to determine their ages and distances with sufficient degree of accuracy (*cf.* Giridhar 1983). The accuracy of these parameters determine the accuracy of the derived birthsites. Also, the young age of classical Cepheids with periods longer than ten days imply that the variations of [Fe/H] observed in the sample is due to the spatial variation of ISM at the current epoch.

Our compilation of spectroscopically derived [Fe/H] abundances of Cepheids is described in Section 2, together with distances and ages. The birthsites are derived in Section 3. The radial abundance gradient and the local chemical inhomogeneities across the spiral arms are estimated in Section 4 and discussed in Section 5.

2. The basic data

2.1 *Spectroscopically Derived [Fe/H] Abundances in Cepheids*

We summarize in Table 1 the compilation of [Fe/H] abundances for different Cepheids, derived by different investigators. The table also contains the basic data for these Cepheids, like the galactic coordinates, the visual magnitudes, periods, distances from the Sun and from the centre of the Galaxy. The abundance estimates used in this compilation are critically discussed below.

Rodgers & Bell (1963) determined the atmospheric abundances of β Dor employing a differential curve of growth with respect to the Sun. The choice of the Sun for differential analysis is not justified due to the difference in gravities. No other abundance determination exists for this star. Bappu & Raghavan (1969) derived atmospheric abundances of RT Aur using the same technique. The standard error of the [Fe/H] determined by them is ± 0.15 dex. Unfortunately, the *gf* values available in the 1960s were later found to be very uncertain, in many cases differences being of several orders of magnitude. As a result we were obliged to exclude from our investigation the [Fe/H] derived prior to 1970.

Van Paradijs & Ruiter (1973) determined [Fe/H] for δ Cep using curve-of-growth and model-atmosphere method, and derived almost a solar value. This is in good agreement with the recent estimates of Luck & Lambert (1981, hereinafter LL) using the spectrum synthesis method.

Schmidt (1971) derived [Fe/H] for four southern Cepheids—η Aql, S Nor, Y Oph and U Sgr— using the curve-of-growth and model-atmosphere method. The effective temperature and surface gravity were determined by matching the observed continuous energy distribution with theoretical fluxes calculated using the model atmosphere. The

Table 1. Compilation of spectroscopic [Fe/H] for Cepheids.

Star	Galactic coordinates l	b	Mag.	Period (days)	Present position $R_\odot$	R_{gc}	[Fe/H]	Source
UZ Sct	19.16	−01.49	12.4	14.744	3.3	6.96	+0.25	8
WZ Sgr	12.10	−01.30	9.0	21.849	2.16	7.89	+0.15	7
CK Sct	26.30	−00.46	10.54	7.40	2.20	8.06	+0.13	8†
S Nor	327.75	−05.39	6.11	9.755	1.00	9.16	+0.10	3
SV Vul	63.94	+00.30	6.73	45.035	2.34	9.20	+0.28	6
Y Oph	20.60	+10.38	7.15	17.123	0.76	9.29	+0.18	3
U Sgr	13.70	−04.45	6.35	6.745	0.68	9.33	+0.10	3
W Sgr	1.60	−04.00	4.70	7.595	0.48	9.52	+0.27	6
X Sgr	1.16	+00.20	4.79	7.012	0.42	9.58	+0.02	6
							+0.07	7
η Aql	40.93	−13.07	4.08	7.176	0.30	9.77	+0.06	6
							+0.08	4
X Cyg	76.87	−04.26	6.65	16.384	1.16	9.80	+0.08	4
							+0.15	6
							+0.33	8
T Vul	72.13	−10.15	5.43	4.435	0.61	9.83	−0.05	6
DT Cyg	76.54	−10.78	6.06	2.499	0.45	9.90	+0.12	6†
β Dor	271.74	−32.78	4.03	9.842	0.36	9.99	+0.01	2*
TX Cyg	84.35	−02.30	10.34	14.708	1.3	10.01	+0.39	8
αU Mi	1.49	89.03	2.0	3.97	0.1	10.05	−0.07	9
δ Cep	105.20	+00.53	4.94	5.336	0.29	10.08	+0.06	6
							−0.06	5
SU Cas	133.47	+08.51	6.38	1.949	0.31	10.21	−0.12	6†
ζ Gem	195.74	+11.89	3.68	10.151	0.39	10.37	+0.34	6
							+0.20	7
RT Aur	183.14	+8.90	5.48	3.728	0.49	10.48	−0.20	1*
							+0.06	6
TU Cas	118.92	−11.40	7.38	2.139	0.93	10.48	−0.13	6†
RS Pup	252.40	−00.20	7.59	41.387	2.08	10.81	−0.07	6
DL Cas	120.26	−02.55	9.72	8.000	1.67	10.94	−0.13	8
T Mon	203.63	−02.56	5.59	27.020	1.42	11.31	+0.12	6
							+0.03	7
							+0.14	4
RX Aur	165.80	−01.30	7.67	11.622	1.98	11.93	−0.37	4
SV Mon	203.63	−03.7	8.30	15.232	2.87	12.68	−0.10	7
BM Per	155.60	−00.09	11.40	22.952	3.0	12.79	−0.10	8
TV Cam	145.00	+06.14	11.76	5.3	5.1	13.63	−0.11	8†
YZ Aur	167.30	+00.93	11.08	18.193	4.5	14.42	−0.26	8

Sources:
1. Bappu & Raghavan (1969)
2. Rodgers & Bell (1963)
3. Schmidt (1971)
4. Schmidt, Rosendhal & Jewsbury (1974)
5. van Paradijs & Ruiter (1973)
6. Luck & Lambert (1981)
7. Giridhar (1983)
8. Harris & Pilachowski (1984)
9. Giridhar (1985)

* Rejected because of uncertain abundances.
† Rejected because of large age and unknown space velocity.

standard error of the abundance estimate is around ± 0.1 dex. The Cepheid η Aql has also been investigated by LL and there is a satisfactory agreement between the two estimates.

Schmidt, Rosendhal & Jewsbury (1974, hereinafter SRJ) derived atmospheric abundances of X Cyg, T Mon and RX Aur using curve-of-growth and model-atmosphere method. The temperature scale for Cepheids was derived from a study of the Hα profile (Schmidt 1972a) and continuum photometry (Schmidt 1972b). For T Mon and X Cyg, the temperatures and gravities determined by SRJ are systematically higher than those derived by Parsons (1970) from six-colour photometry, by Pel (1978) from narrow band *VBLU W* photometry, and also the spectroscopic estimates of LL. The differences are of the order of $\Delta T_{\rm eff} \sim 500$ K and $\Delta \log g \sim 1.6$, and therefore would lead to systematic differences of 0.1 to 0.2 dex in the derived abundances. It is therefore surprising that Fe/H derived by SRJ for T Mon and X Cyg agree with those of LL within 0.15 dex. Yet, we will use with caution the low value of [Fe/H] = −0.37 derived by SRJ for RX Aur.

LL derived atmospheric abundances for 14 Cepheids using the method of spectrum synthesis. The method involves detailed computation of the spectral region of interest using a suitable model atmosphere and atomic parameters of concerned lines. They have employed a large number of iron lines observed with high resolution. The internal error in the determination is 0.06 dex. These estimates are perhaps among the more accurate ones.

Giridhar (1983) derived atmospheric abundances of five Cepheids SV Mon, T Mon, ζ Gem, X Sgr and WZ Sgr. The method employed is similar to LL and there is a good agreement between the two estimates for the stars in common (T Mon, ζ Gem and X Sgr).

Harris & Pilachowski (1984 hereinafter HP) derived [Fe/H] for YZ Aur, TV Cam, DL Cas, BM Per, TX Cyg, X Cyg, CK Sct and UZ Sct using high-dispersion spectra and fine analysis. However, for X Cyg the estimate of HP is higher than the one derived by LL by 0.18 dex which is surprising. The differences in phases can partly account for the discrepancy. The observations of HP were made at a phase at which the assumption of hydrostatic equilibrium holds better than at the phase observed by LL. Since the internal errors in the abundance estimate of X Cyg and TX Cyg are higher than for other stars of the sample of HP, we have given equal weight to the estimates [Fe/H] derived by LL, HP and SRJ.

2.2 *Distances to the Cepheids*

The most commonly used relationships for determination of distances to Cepheids are the period-luminosity-colour (*P-L-C*) relationships of Sandage & Tammann (1969) and Tammann (1970). With this method, the accuracy of the derived distance depends upon the accuracy with which the colour excess is determined. Early determination of the colour excesses using *UBV* photometry showed large systematic differences between various estimates that depended on the periods and also on the amount of reddening. We now know that the broadband photometric systems like *UBV* are not suitable for the colour-excess determination because the derived colour excess depends upon the stellar energy distribution. In the case of Cepheids the situation is further complicated by the variation of spectral type over the pulsation cycle.

Recent determination of colour excesses of a large number of Cepheids by Pel (1978) using narrow-band *VBLU W* photometry, by Parsons & Bell (1975) using six-colour *UVBGRI* photometry, and by Dean, Warren & Cousins (1978) using *BVI* photometry, show a satisfactory agreement between themselves. Not only are the systematic

differences very small, but also they are independent of period. However, all these colour excess estimates differ systematically from the older estimates (*e.g.*Kraft 1961) that used broad band photometry, in the sense that the former indicate a smaller value of colour excess. The calibration of *P-L-C* relation of Sandage & Tammann (1969) was done using the colour excesses derived by Kraft (1961) and therefore requires recalibration.

Another recent attempt to determine accurate distances to Cepheids is made by Barnes, Evans & Parsons (1977). These authors used the surface brightness inferred from the $(V-R)$ colour index to determine the variation in the angular dimension of Cepheids. By combining the data with linear displacements derived from the radial velocity curves, the distances and the linear radii are determined. The distances derived by Barnes *et al.* are systematically larger by about 18 per cent compared to those derived by Tammann (1970).

We have used the *P-L-C* relationship of Caldwell (1983) to derive the distances of Cepheids. Caldwell considered 22 Cepheids that are members of galactic clusters and used for reddening correction the colour excesses derived by Pel (1978), Parsons & Bell (1975) and Dean, Warren & Cousins (1978). The attractive feature of this relationship is a better agreement with the methods that do not employ estimates of cluster distances (*e.g.* Barnes, Evans & Parsons 1977).

We have taken the mean magnitudes $\langle B \rangle$ and $\langle V \rangle$ for the sample Cepheids from Schaltenbrand & Tammann (1970). The heliocentric distances derived using the *P-L-C* relation of Caldwell are given in Table 1. The standard error in distances derived are ± 10 per cent.

2.3 *Ages of the Cepheids*

If the age of a star is known, one can compute its galactic orbit backwards in time and derive its birthsite. The age of a Cepheid can be inferred from its period–age relationship (Hodge 1961; Efremov 1964). A theoretical period–age relationship for classical Cepheids was derived by Kippenhahn & Smith (1969) from stellar evolutionary calculations. Tammann (1970) gave an analytical representation to the results of Kippenhahn & Smith for a stellar model with a composition of $X = 0.602$ and $Z = 0.044$ as

$$\log \tau_7 = 1.16 - 0.651 \log P,$$

where τ_7 is the age in 10^7 yr and P is the period in days. Efremov (1978) derived a composite period–age relationship from the data on a large number of Cepheids belonging to clusters and associations in Magellanic Clouds, the Galaxy and M 31 as

$$\begin{gathered}\log \tau_7 = 1.157 - 0.677 \log P \\ \pm 0.37 \quad \pm 0.47\end{gathered}$$

for 2d $< P <$ 50d. This relation agrees closely with the theoretical relation. We have listed in Table 2 the ages calculated using the semi-empirical relationship of Efremov (1978), for cepheids with $P > 3$d. These ages are systematically smaller by 0.25×10^7 yr compared to the ages calculated by Wielen (1973) using the theoretical relationship of Kippenhahn & Smith. After considering the spread in chemical composition for the sample Cepheids, the random errors in the derived ages of Cepheids are estimated to be less than ± 30 per cent.

Table 2. Ages, present positions, and birthsites for the sample Cephieds.

S. No.	Star	Age 10^7 yr	[Fe/H]	Present position ξ	η	ζ	birthsite in ω_p system ξ_p	η_p	R_{gc}	spiral feature Th	obs
1	UZ Sct	2.33	+0.25	3.11	1.08	−0.08	3.48	−2.52	6.99	—	C
2	WZ Sgr	1.78	+0.15	2.12	0.05	−0.04	2.19	−0.88	7.85	S	S
3	S Nor	3.07	+0.10	0.84	−0.53	−0.09	2.47	−3.88	8.47	S	S
4	SV Vul	1.09	+0.28	1.03	2.09	+0.01	0.45	+0.75	9.58	—	L
5	Y Oph	2.09	+0.18	0.70	0.26	+0.14	0.88	−2.11	9.36	—	S
6	U Sgr	3.94	+0.10	0.66	0.16	−0.05	1.60	−4.40	9.48	S	S
7	W Sgr	3.63	+0.27	0.47	0.01	−0.03	2.12	−5.34	9.52	S	S
8	X Sgr	3.80	+0.05	0.42	0.01	+0.00	1.90	−4.68	9.35	S	S
9	η Aql	3.78	+0.07	0.22	0.19	−0.07	1.54	−4.30	9.49	S	S
10	X Cyg	2.16	+0.19	0.26	1.13	−0.08	−0.62	−1.52	10.73	—	L
11	T Vul	5.23	−0.05	0.18	0.57	−0.11	1.18	−5.34	10.31	—	S
12	α UMi	5.90	−0.07	0.10	−0.05	0.08	3.37	−6.04	8.67	—	S
13	TX Cyg	2.33	+0.39	0.13	1.29	−0.05	−0.26	−1.19	10.33	—	L
14	δ Cep	4.62	+0.00	−0.07	0.29	−0.01	1.51	−4.55	9.63	—	S
15	ζ Gem	2.99	+0.27	−0.38	−0.01	0.08	−0.11	−3.77	10.81	—	—
16	RT Aur	5.90	+0.06	−0.48	−0.03	0.07	+3.19	−5.77	8.92	S	S
17	RS Pup	1.15	−0.07	−0.63	−1.98	−0.01	2.20	−4.28	8.89	S	S
18	DL Cas	3.51	−0.13	−0.84	1.44	−0.07	−0.91	−1.94	11.08	P	L
19	T Mon	1.54	+0.10	−1.29	−0.56	−0.06	−0.90	−1.54	11.01	P	L
20	RX Aur	2.73	−0.37	−1.92	+0.49	−0.04	−0.57	+1.49	10.67	P	—
21	SV Mon	2.27	−0.10	−2.62	−1.15	−0.18	−1.97	+1.72	12.09	P	P
22	BM Per	1.72	−0.10	−2.73	1.24	−0.00	−2.74	+0.26	12.73	P	P
23	YZ Aur	2.01	−0.26	−4.39	0.99	+0.07	−4.38	+0.57	14.40	—	—

3. Places of formation of Cepheids

3.1 *Computation of Galactic Orbits*

The birthsites of the Cepheids were derived by computing their galactic orbits backwards in time until the time of their birth. For axisymmetric gravitational field we have used the recent expression of Contopoulos as given by Palous *et al.* (1977):

$$\Psi_0 = \text{constant} + \frac{3000}{R} - 10120.2\ R + 13.9073R^3, \qquad R < 9.732175$$

$$\Psi_0 = -402667.526\left[-\frac{(R^2-94.4784)^{1/2}}{2R^2} + 0.0514403\ \cos^{-1}\frac{9.72}{R}\right]$$

$$-\frac{97970.75}{R^2} + \frac{30000}{R} + 15.029[R^3 - (R^2-94.4784)^{3/2}]$$

$$-10625.75R + 8522.87619[(R^2-94.4784)^{1/2} - 9.72\ \cos^{-1}\frac{9.72}{R}],$$

$$R > 9.732175,$$

where R is in kpc. For stars close to the Sun ($R \sim 10$ kpc) the birthsites derived using the expression of Contopoulos & Strömgren (1965) for Ψ_0 and the recent expression mentioned above do not differ significantly. However, in our sample we have stars up to galactocentric distance $R = 14.4$, and hence the use of the new expression of Contopoulos was considered necessary.

For the potential of spiral field the analytical approximation of density wave by a logarithmic spiral and the set of parameters derived by Yuan (1969) were adopted. The equation of motion in (ξ, η, ζ) coordinate system is given by

$$\ddot{\xi} + 2\,\omega_0\dot{\eta} + \omega_0^2(R-\xi) = \frac{d\Psi}{d\xi},$$

$$\ddot{\eta} - 2\,\omega\dot{\xi} - \omega_0^2\eta = \frac{d\Psi}{d\eta},$$

$$\ddot{\zeta} = \frac{d\Psi}{d\zeta}.$$

The origin of this system rotates around the galactic centre with an angular velocity $\omega_0 = 25\,\text{km s}^{-1}\,\text{kpc}^{-1}$ at a distance $R = 10$ kpc from the galactic centre, the ξ axis reckoned positive towards the galactic centre, the η axis in the direction of galactic rotation, and the ζ axis towards the galactic pole. These equations were numerically integrated using the Runge–Kutta method. A time step of 0.5×10^6 yr was employed.

This coordinate system of reference does not give any insight into the influence of density wave on star formation. The birthsites are hence transformed into ω_p reference system which corotates with density wave and hence gives the location of the birthsites with respect to the density wave. We have listed in Table 2 the birthsites (ξ_p, η_p) in the ω_p system.

The space velocities used in the present investigation are derived by Giridhar (1986) using the proper motion data of Karimova & Pavlovskaya (1981). These proper

motions are calculated using a number of new position catalogues and some new observations obtained with Repsoid meridian circle at the observatory of Moscow and are more accurate (0.0005 s yr^{-1} in μ_α and 0.005 arcsec yr^{-1} in μ_δ) compared to the ones used by Wielen (1974) to derive the space velocity components. Owing to the large uncertainty in the proper motions, the space velocity components were not derived by Wielen (1974) for the cepheids farther than 1 kpc. For distant Cepheids like RS Pup, WZ Sgr, T Mon, X Cyg *etc.* which are young, the birthsites were calculated by Wielen (1973) assuming the space velocity components to be zero. However, the space velocity components are calculated by Giridhar (1986) for these distant Cepheids using the current proper motion estimates of Karimova & Pavlovskaya (1981). As a result, we have used the space velocity components in the birthsite calculations for the majority of the Cepheids in our sample. Only for three Cepheids (UZ Sct, BM Per, and YZ Aur) the proper motions, and therefore the space velocity components, were not available. Since all the three Cepheids are younger than 2.3×10^7 yr and could not have moved considerably from their birthsites, we felt justified in calculating their birthsites with the assumption of zero space velocities. We have omitted CK Sct and TV Cam of Table 1 from our sample because the space velocity components were not available for them and their ages are too large to validate the assumption of zero space velocity.

3.2 *Error Analysis*

The observed parameters that are used in birthsite determinations are the distances, the space velocity components, and ages. Amongst these, the distances are known to an accuracy of $\pm$ 10 per cent. As a typical example if we consider ζ Gem, then a random error of 10 per cent in the distance corresponds to an uncertainty of $\sim$ 0.05 kpc in ξ_p and 0.015 kpc in η_p, in ω_p system. The random errors in ages of the Cepheids are estimated to be $\sim$ 20 to 30 per cent. For ζ Gem a random error of 25 per cent in age led to an uncertainty of 0.07 kpc in ξ_p and 0.56 kpc in η_p. The errors in space velocities do not affect the birthsites significantly. An error of 5.0 km s^{-1} in U and V space velocity components only caused an error of 0.25 kpc over the time span of 3.0×10^7yr. It is due to the fact that the differences between the circular velocity of stars (250 km s^{-1} in solar neighbourhood) and density-wave velocity ($\sim$ 135 km s^{-1}) which is around 115 km s^{-1} is much larger than the peculiar velocities of the stars.

Since the birthsites are found to depend more strongly on the ages than on other parameters, we have limited our sample to the age range 1.2–5.5 $\times 10^7$ yr. The Cepheids DT cyg, SU Cas and TU Cas were dropped from the sample because their ages (8–9 $\times 10^7$ yr) were outside this range.

4. Local chemical inhomogeneities

We plot in Fig. 1 [Fe/H] as a function of present galactocentric distance for the Cepheids of Table 1. Some of the stars of Table 1 were rejected from the sample either due to very uncertain abundance estimates or due to the larger ages and absence of space velocity components for them. The rejected stars are marked in the table. Though we intended to keep the sample age to 5.5 $\times 10^7$ yr we have retained slightly older α UMi and RT Aur in this study, since precise proper motion and hence space velocity

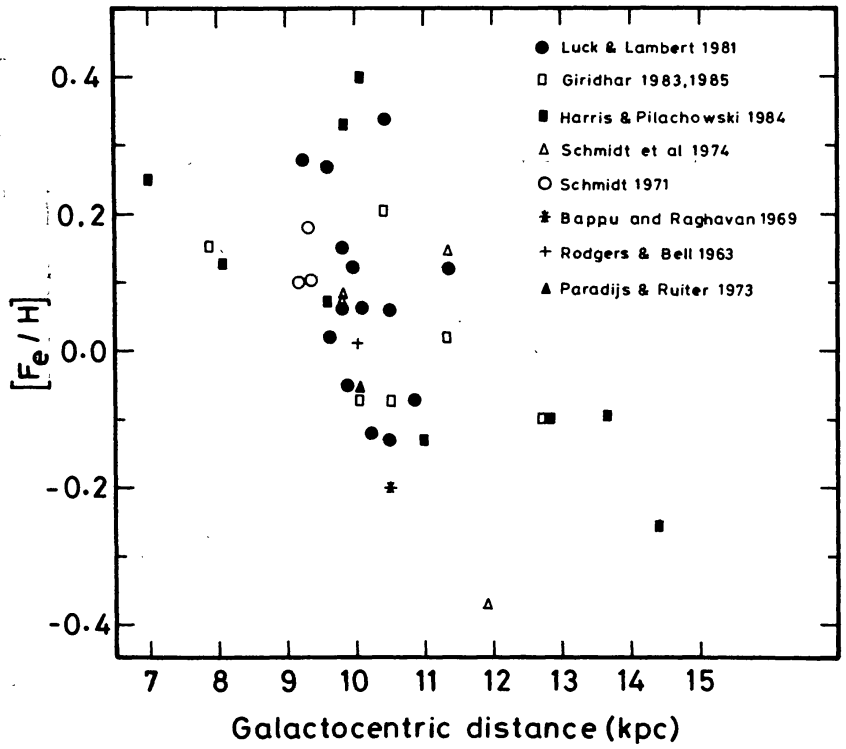

Figure 1. A plot of [Fe/H] as a function present galactocentric distances for the Cepheids of Table 1.

components are available for them (due to their small distances from the Sun). A straightline fit to the accepted data points of Table 1 gives

$$[\mathrm{Fe/H}] = 0.83 - 0.074 R_{gc} \quad (n = 31,\ r = 0.61)$$
$$\pm 0.24 \pm 0.018$$

The gradient agrees reasonably well with the earlier values derived by Luck (1982), Giridhar (1983), Harris & Pilachowski (1984) and others. The stars TXCyg, RX Aur and ζ Gem lie beyond 2σ of this line and provide the first hint that there are smallscale variations superposed on global radial abundance gradient.

We have shown in Fig. 2 the places of formation in ω_p system for the stars in Table 2. The spiral arms are shown as bands corresponding to a positive excess of density in the model of Yuan (1971). The figure shows the sagittarius arm (S) and the Perseus arm (P). We have divided the observed metallicities of Cepheids into four groups:

(1) metal poor	$[\mathrm{Fe/H}] < -0.10,$
(2) solar	$-0.10 < [\mathrm{Fe/H}] < +0.10,$
(3) Marginally rich	$0.10 < [\mathrm{Fe/H}] < +0.20,$
(4) Metal rich	$[\mathrm{Fe/H}] > 0.20.$

Different symbols are used for stars belonging to different groups. The stars are identified in the figure by the serial numbers in Table 2.

The tightly wound theoretical spiral pattern (pitch angle 6°) of Yuan, which was derived with an aim to explain the grand design of whole disc, fitted very well with major spiral arms like the Sagittarius and Perseus arms, but not with the Orion feature.

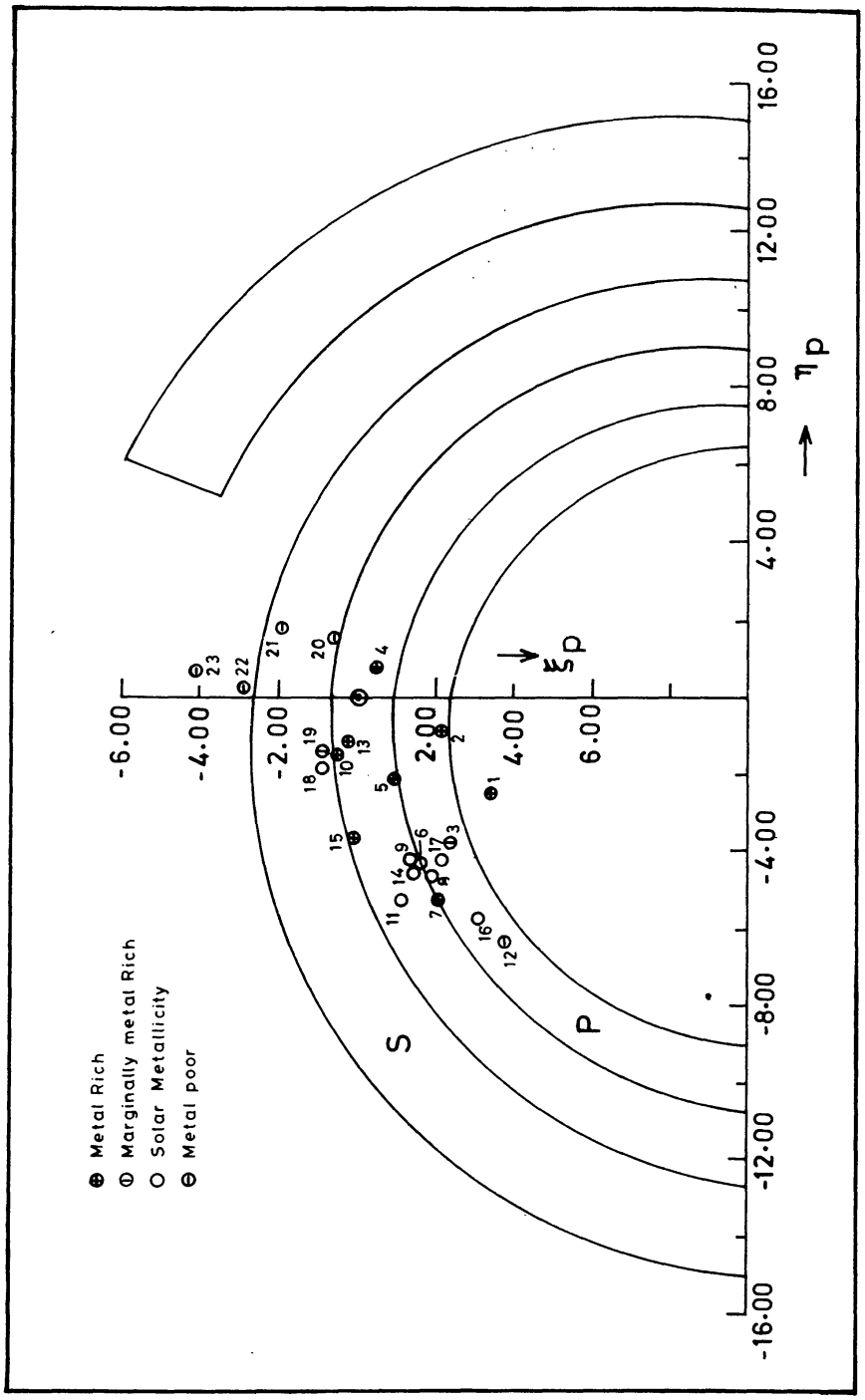

Figure 2. The distribution of the birthsites in ω_p system. The spiral arms are from the density-wave model of Yuan (1971). Sun's position is shown by ⊙ symbol.

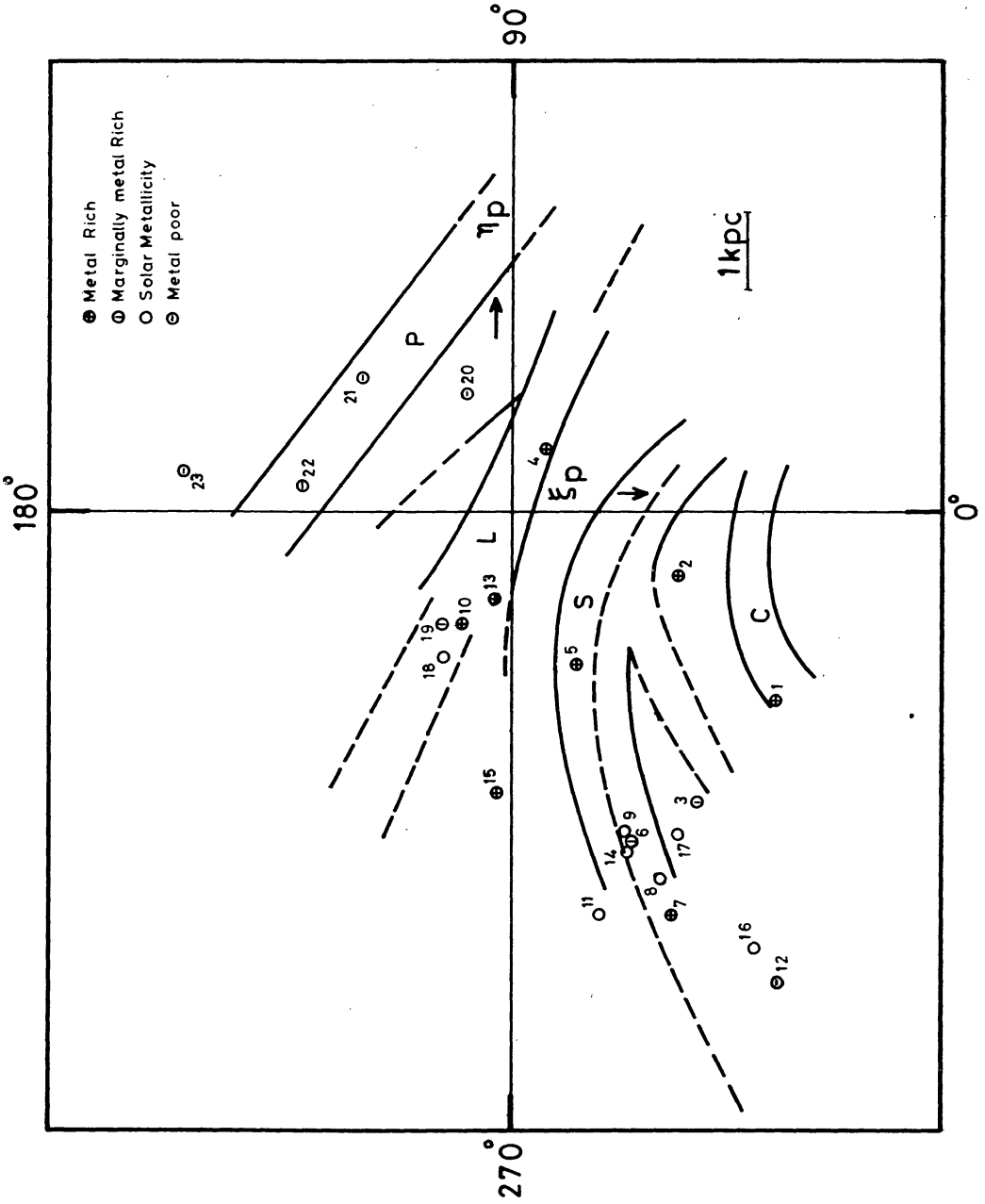

Figure 3. The distribution of the places of formation of the sample stars in the galactic plane. The outline of the optical spiral feature are taken from Humphreys (1979).

It is of interest to consider the observed spiral features traced by HII regions and young, active stellar associations. We now plot in Fig. 3 the birthsites superposed on the observed spiral features given by Humphreys (1979). The figure shows four main spiral features, the Carina arm (C), the Sagittarius arm (S), the Local arm (L) and Perseus arm (P).

We have indicated in the last column of Table 2 the assignment of Cepheids to different spiral arms. The spiral arms shown in Figs 2 and 3 are treated separately. We plot in Fig. 4 (a) and (b) the [Fe/H] values of Cepheids from Table 2 as a function of the galactocentric distances of their birthsites. The Cepheids belonging to the Sagittarius and Perseus arms are shown by different symbols, and the ones that belong to neither, by a third symbol. The lone Cepheid belonging to the 'observational' Carina feature is pooled with the Sagittarius Cepheids. The local feature is treated as the interarm region.

A least-squares fit to the entire data in Fig. 4 gives

$$[\mathrm{Fe/H}] = 0.59 - 0.054\, R_{gc} \qquad (n = 23,\ r = 0.48)$$
$$\pm 0.29 \pm 0.022$$

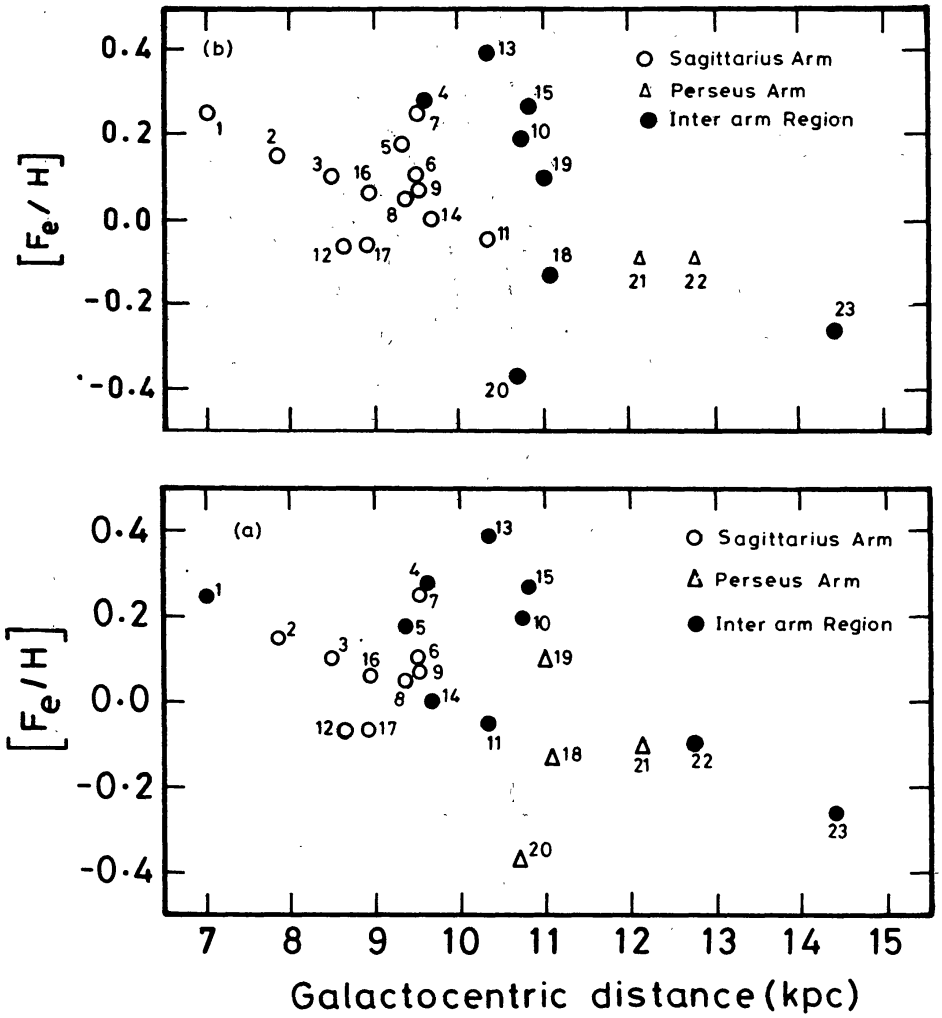

Figure 4. A plot of [Fe/H] for the stars of Table 2 as a function of galactocentric distances of their birthsites: (a) spiral-arm assignment based on Fig. 2; (b) spiral-arm assignment based on Fig. 3.

However, there is a large scatter in the region 9–11 kpc where several metal-rich interarm/local-feature Cepheids exist. Considering only the Sagittarius and Perseus Cepheids, one obtains for Fig. 4 (a)

$$[\mathrm{Fe/H}] = 0.58 - 0.059\ R_{gc} \qquad (n = 12,\ r = 0.45)$$
$$\pm 0.79 \pm 0.035$$

and for Fig. 4(b)

$$[\mathrm{Fe/H}] = 0.55 - 0.052\ R_{gc} \qquad (n = 15,\ r = 0.62).$$
$$\pm 0.30 \pm 0.018$$

The scatter in metallicities of the major-arm Cepheids corresponds to standard deviations of 0.15 and 0.09 for the theoretical and observational spiral features. On the other hand, the scatter in the metallicities of the remaining Cepheids about the line defined by the major-arm Cepheids is much higher, 0.20 and 0.26, respectively. An *F*-test shows that the two sample standard deviations differ with a probability of 85 per cent and 99 per cent respectively, for the theoretical and observational spiral features. Furthermore, the local arm and the interarm Cepheids are overabundant by 0.15 (0.09) dex, a value, though not statistically significant, yet highly suggestive.

We had remarked in Section 2 that the abundance estimate of RX Aur needs to be used with caution. This star falls in the Perseus arm in Fig. 2 and in the interarm region in Fig. 3. Its exclusion changes the gradient based on the major arm stars of Fig. 2 to a somewhat shallower value. Though its exclusion reduces the scatter, the significance levels of *F*-test do not change appreciably. On the other hand, the mean abundance of interarm and local feature Cepheids (based on Fig. 3) now increases to 0.15 dex, in agreement with the value based on Fig. 2.

Ascribing the spread in the abundances of the Cepheids in Sagittarius and Perseus arms to the errors of determination, we obtain an intrinsic spread of 0.14–0.24 dex for the interarm Cepheids, depending on whether one considers the spiral arms in Fig. 2 or Fig. 3.

5. Discussion

The observations of local chemical inhomogeneities have important implications for the models of star formation as well as galactic chemical evolution. The models of these two aspects of galactic evolution have been made in the past fairly independently, and under simplifying assumptions.

One of the popular star formation models is based on the density wave in which star formation is triggered only when the disc gas encounters the density-wave pattern and is compressed in a shock region near the wave-crest (Roberts 1969). Jensen, Strom & Strom (1976) were able to explain the radial abundance gradients observed in several galaxies using the density-wave model.

The simple models of galactic evolution which predict a smooth radial abundance gradient (in agreement with observations) assume that the star formation takes place in isolated well-mixed zones, *i.e.*, there is no variation of metallicity in these zones. A detailed study of the efficiency of various mixing processes in the disc of our Galaxy is made by Edmunds (1975). He demonstrated that over the timescale of 2×10^8 yr, which is the time interval between two successive passages of density wave, the chemical

inhomogeneities in ISM, produced by processed gas ejected by massive stars would get mixed with ISM. Over this timescale, the turbulent velocities in ISM will cause a mixed length of $\sim$ 300 pc. The shear due to differential rotation (at solar distance) will cause the mixing to spread over a volume of 1.1×10^{11} pc^3. All these effects will dilute the inhomogeneity to $\Delta Z = 9 \times 10^{-5}$ by the time star formation due to density wave recurs in the same place.

Stochastic self-propagating star-formation model is an alternative which suits late-type galaxies with less well-defined spiral arms (Gerola & Seiden 1978). SPSF models assume the expanding shells of supernova remnants or HII regions to furnish the necessary compression at their edges where the stars would consequently form. Stars are formed in the expanding shell after the expansion velocity of the shell becomes comparable to the turbulent velocities in ISM. The massive stars among the newly born produce more such shells and thus the process propagates. The propagation of star formation process is controlled by the refractory period τ_r which is the minimum time before a given cell can undergo star formation again. The refractory period is the length of time it takes for the gas density at a given location to build up after the location has experienced a supernova. In the case of pure SPSF models the refractory period (1.6×10^8 yr) for a given region is again too large for the chemical inhomogeneities to survive before the star formation resumes. Mueller & Arnett (1976) introduced density waves in their SPSF models and found the regeneration time to decrease by a factor of 2–3. This provides for the possibility of forming second-generation stars before the chemical inhomogeneity is fully diluted.

A gas-dynamical model of ISM in the Galaxy is developed by Roberts (1982) with an aim to arrive at a better understanding of global (such as density-wave induced) as well as local processes of star formation active in the Galaxy, and their relationship with each other. Roberts employs a time delay rT_D before an active stellar association forms from colliding clouds and a time delay of $r'_D T'_D$ before the clouds could interact with associations to produce stars. Here T_D and T'_D represent the maximum probabilistically-selected delay times, and r and r' are the random numbers selected between zero and unity for each association. Roberts found that $T_D = T'_D = 0$ resulted in well-delineated spiral arms whereas $T_D = T'_D = 2 \times 10^7$ yr yielded arms with spurs.

The spread in metallicity of galactic stars of a given age, observed by Dixon (1966) and Hearnshaw (1972), indicates that the ISM is not well-mixed throughout the galactic disc and spatial variation of metallicity exists. The local chemical inhomogeneity reported by Talent & Dufour (1979) and also the one observed in the present work strengthens the view that the mixing of ISM in different zones of galactic disc is not complete. On the other hand, the shell of cold HI, dust and molecules around supernova remnants detected by Sancisi (1974) and Knapp & Kerr (1974), and young stellar associations on the edge of supernova shells observed by Berkhuijsen (1974) and Herbst & Assoussa (1978), indicate the existence of a secondary process of star formation.

We now attempt to link these two observations in the light of what we have learnt from the models of star formation. The two observations, taken together, require that the time delay between two star-formation events is neither too large as implied by the density-wave model, nor too small as the zero-time-delay model of Roberts (1982). A time delay of 4–5 $\times 10^7$ yr appears consistent with the model of Roberts (1982) as well as Mueller & Arnett (1976). Over this timescale, the gas enriched by supernovae in Sagittarius arm would move over to the region corresponding to the local feature.

As Edmunds (1975) points out, a value of $\Delta Z \sim 4 \times 10^{-3}$ may be expected between

the inside and outside of a composite supernova shell around a typical OB association of 60 pc size containing 15 O-B2 stars. It is conceivable that this gas stays undiluted due to snowplough effect when the shell encounters high density gas. Radio observations of Perseus gas cloud by Sancisi (1974) indicate the presence of an expanding shell of HI. Sancisi (1974) estimated the radius and thickness of the shell to be 20 pc and 5 pc respectively, and suggested that it contains $10^4 M_\odot$ of gas. If it contains the $90 M_\odot$ of metals injected by 15 SN of a typical OB association, one would expect an enrichment of $\Delta Z \sim 9 \times 10^{-3}$. Over the time interval of 5×10^7 yr the mixing-length resulting due to turbulent eddies is 130 pc (*cf.* Edmunds 1975). This will lead to a mixed gas of mass $6 \times 10^4 M_\odot$, if we adopt for the density near the galactic plane a value of $0.018 M_\odot$ pc^{-1} (Allen 1973). Consequently, the metallicity will be diluted to $\Delta Z \sim 1.3 \times 10^{-3}$. This corresponds to an enrichment of 0.1 dex in Fe/H considering its contribution to be 0.014 to the total metallicity. It is possible that there would be more than one generation of star-formation in the spiral arm itself($rT_D \simeq rT'_D \simeq 0$). Also, the enhancement of metals may be retained with less dilution when SN shell interacts with neighbouring shells rather than the unenriched ISM. Consequently, even higher chemical enrichment is possible. Thus it would appear that enhanced star formation in the major spiral arms, and secondary star-formation in the minor interarm features such as the local arm—when the fossil SN shell fragments to form stars—may explain the observed metallicity variations adequately.

Acknowledgements

I wish to thank Dr T. P. Prabhu for many useful discussions and two anonymous referees for comments.

References

Allen, C. W. 1973, *Astrophysical Quantities*, 3 edn, Univ. London, Athlone Press.
Bappu, M. K. V., Raghavan, N. 1969, *Mon. Not. R. astr. Soc.*, **142,** 295.
Barnes, T. G., Evans, D. S., Parsons, S. B. 1976, *Mon. Not. R. astr. Soc.*, **174,** 503.
Berkhuijsen, E. M. 1974, *Astr. Astrophys.*, **35,** 429.
Caldwell, J. A. R. 1983, SAAO Preprint No. 336.
Contopoulos, G., Strömgren, B. 1965, *Tables of Plane Galactic Orbits*, Institute of Space Studies, New York.
Dean, J. F., Warren, P. R., Cousins A. W. J. 1978, *Mon. Not. R. astr. Soc.*, **183,** 569.
Dixon, M. E. 1966, *Mon. Not. R. astr. Soc.*, **131,** 325.
Edmunds, M. G. 1975, *Astrophys. Space Sci.*, **32,** 483.
Efremov, Yu, N. 1964, *Perem. Zvezdy*, **15,** 242.
Efremov, Yu, N. 1978, *Sov. Astr.*, **22,** 161.
Gerola, H., Seiden, P. E. 1978, *Astrophys. J.*, **223,** 129.
Giridhar, S. 1983, *J. Astrophys. Astr.*, **4,** 75.
Giridhar, S. 1985, in *IAU Coll.* 82: *Cepheids: Theory and Observation*, Eds B. F. Madore, Cambridge Univ. Press, p. 100.
Giridhar, S. 1986, In preparation.
Grivnev, E. M. 1983, *Sov. Astr. Lett.* **9,** 287.
Grosbøl, P. J. 1977 in *IAU Coll.* 45: *Chemical and Dynamical Evolution of our Galaxy*, Eds E. Basinska-Grzesik & M. Mayer, Geneva Obs., p. 279.
Harris, H. C., Pilachowski, C. A. 1984, *Astrophys. J.*, **282,** 655 (HP).
Herbst, W., Assousa, G. E. 1978, in *Proto Stars and Planets*, Ed. T. Gehrels, Univ. Arizona Press, Tucson, p. 368.

Hearnshaw, J. B. 1972, *Mem. R. astr. Soc.*, **77,** 55.
Hodge, P. W. 1961, *Astrophys. J.*, **133,** 64.
Humphreys, R. M. 1979 in *IAU Symp.* 84: *The Large-Scale Characteristics of the Galaxy*, Ed. W. B. Burton, D. Reidel, Dordrecht, p. 93.
Joshi, U. C. 1982, *Bull. astr. Soc. India*, **10,** 271.
Jensen, E. B., Strom, K. M., Strom, S. E. 1976, *Astrophys. J.*, **209,** 748.
Kippenhahn, R., Smith, L. 1969, *Astr. Astrophys.*, **1,** 142.
Karimova, D. K., Pavlovskaya, E. D. 1981, *Sov. Astr. Lett.*, **7,** 61.
Knapp, G. R., Kerr, F. J. 1974, *Astr. Astrsophys.*, **33,** 463.
Kraft, R. P. 1961, *Astrophys. J.*, **134,** 616.
Luck, R. E. 1982, *Astrophys. J.*, **256,** 177.
Luck, R. E., Lambert, D. L. 1981, *Astrophys. J.*, **245,** 1018 (LL).
Mueller, M. W., Arnett, W. D. 1976, *Astrophys. J.*, **210,** 670.
Palous, J., Ruprecht, J., Dluzhnevskaya, O. B., Pikunov, T. 1977, *Astr. Astrophys.*, **61,** 27.
Parsons, S. B. 1970, *Bull. Am. astr. Soc.*, **2,** 334.
Parsons, S. B., Bell, R. A. 1975, *Dudley Obs. Rep. No.* 9.
Pel, J. W. 1978, *Astr. Astrophys.*, **62,** 75.
Roberts, W. W. 1969, *Astrophys. J.*, **158,** 123.
Roberts, W. W. 1982, in *Kinematics, Dynamics, and Structure of the Milky Way*, Ed. W. L. H. Shutter, D. Riedel, Dordrecht, p. 265.
Rodgers, A. W., Bell, R. A. 1963, *Mon. Not. R. astr. Soc.*, **125,** 487.
Sancisi, R. 1974, in *IAU Symp.* 60: *Galactic Radio Astronomy*, Eds F. J. Kerr & S. C. Simonson, III, D. Reidel, Dordrecht, p. 115.
Sandage A., Tammann, T. A. 1969, *Astrophys. J.*, **157,** 683.
Schaltenbrand, R., Tammann, G. A. 1971, *Astr. Astrophys. Suppl. Ser.*, **4,** 265.
Schmidt, E. G. 1971, *Astrophys. J.*, **170,** 109.
Schmidt, E. G. 1972a, *Astrophys. J.*, **174,** 595.
Schmidt, E. G. 1972b, *Astrophys. J.*, **174,** 605.
Schmidt, E. G, Rosendhal, J. D., Jewsbury, C. P. 1974, *Astrophys. J.*, **189,** 293.
Strömgren, B. 1967, in *IAU Symp.* 31: *Radio Astronomy and the Galactic System*, Ed. H. van Woerden, Academic Press, London, p. 323.
Talent, D. L., Dufour, R. J. 1979, *Astrophys. J.*, **233,** 888.
Tammann, G. A. 1970, in *IAU Symp.* 38: *The Spiral Structure of Galaxy*, Eds W. Beckers & G. Contopoulos, D. Reidel, Dordrecht, p. 236.
van Paradijs, T. A. 1971, *Astr. Astrophys.*, **11,** 299.
Wielen, R. 1973, *Astr. Astrophys.*, **25,** 285.
Wielen, R. 1974, *Astr. Astrophys. Suppl. Ser.*, **15,** 1.
Yuan, C. 1969, *Astrophys. J.*, **158,** 889.
Yuan, C. 1971, *Astrophys. J.*, **76,** 664.